

# Wafer level self-assembly of microstructures using global magnetic lifting and localized induction welding

Hsueh-An Yang<sup>1</sup>, Chiung-Wen Lin<sup>2</sup> and Weileun Fang<sup>1,2</sup>

<sup>1</sup> Power Mechanical Engineering Department, National Tsing Hua University, Hsinchu 30043, Taiwan

<sup>2</sup> MEMS Institute, National Tsing Hua University, Hsinchu 30043, Taiwan

E-mail: [fang@pme.nthu.edu.tw](mailto:fang@pme.nthu.edu.tw)

Received 7 September 2005, in final form 2 November 2005

Published 7 December 2005

Online at [stacks.iop.org/JMM/16/27](http://stacks.iop.org/JMM/16/27)

## Abstract

This study has successfully demonstrated a process to localize, assemble and weld microstructures using an external magnetic field. The primary three merits of this technology are as follows. (1) The magnetic field is not only to assemble the microstructures but also to fix them by induction welding. (2) The assembly and welding can be localized by the magnetic film. However, a global wafer level process can be achieved by the magnetic field. (3) It is easy to tune the heating temperature by varying the area of the magnetic film; in other words, photolithography can define various temperature regions on a substrate.

(Some figures in this article are in colour only in the electronic version)

## 1. Introduction

There are various available thin film deposition technologies, such as chemical vapor deposition, physical vapor deposition and electroplating. The processing temperature is one major consideration during the integration of microfabrication processes. In addition, the stiffness of micromachined structures is influenced by the thickness of the deposited film. The low temperature electroplating process is regarded as one of the promising fabrication technologies. It is easy to integrate with other processes such as CMOS process. Moreover, the electroplated metal film has the advantages of large thickness and low residual stresses. Thus, the stiffness of the electroplated metal film can be significantly improved. Presently, the electroplated metal film has become one of the promising materials for MEMS devices. Various devices [1] and fabrication platforms [2] using the electroplated metal film have been presented.

It is difficult to produce highly 3D structures using the planar micromachining process. Hence, the applications of MEMS devices are limited. Micro-actuators have been employed to lift up as well as to position micromachined structures to accomplish 3D devices [3]. Moreover, various approaches such as residual stress of thin film [4], magnetic

force [5], ultrasonic wave [6], and solder reflow [7] have also been adopted to assemble micromachined structures after fabrication. In this regard, the locking mechanism is often required to place the micromachined structure at the desired position after assembly [8]. Many of these existing approaches require additional fabrication processes and actuators.

The goal of this study is to realize 3D micromachined metal structures. After the electroplated process, a global magnetic field was used to lift up the movable planar metal microstructures on the wafer. Instead of using the existing locking mechanisms, the induction heating effect by the magnetic field was employed to locally weld the lift-up structure at the proper positioning. In short, 3D micromachined metal structures are implemented by merely using the magnetic field.

## 2. Concept

This study intends to fabricate 3D micromachined metal structures. These metal structures are prepared using a LIGA-like processes, including photolithography, electroplating and etching. As shown in figure 1, the concept of this study is to apply a global magnetic field to lift up the micromachined metal structures on the wafer. In the meantime, the

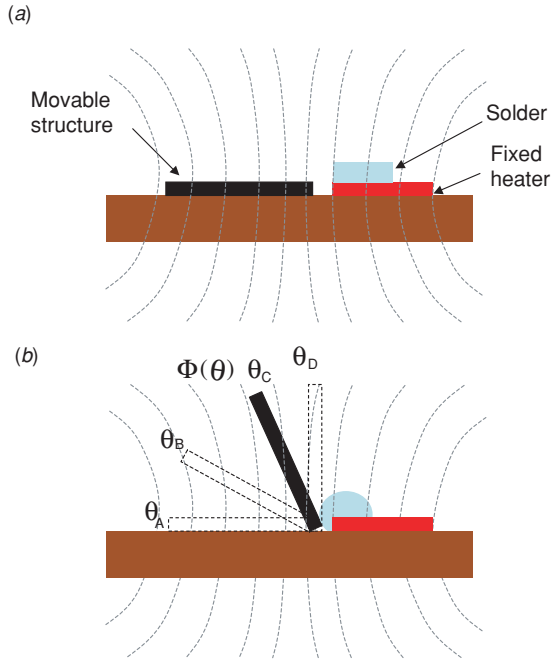


**Figure 1.** The concept of this study is to apply a magnetic field to lift up the movable micromachined metal structures on the wafer, and then to locally weld the lifted structure by the induction-heated solder.

magnetic film at some particular position is heated up by the field according to the induction heating effect [9]. This characteristic has been employed to localize melting the solder in figure 1. The structure lifted up by the magnetic field is designed to contact the melting solder, so that it will be welded to the solder after cooled. Thus, the metal structures are assembled and locked simultaneously when applying the magnetic field. The wafer level self-assembly of metal microstructures can be achieved.

The torque  $T_{\text{field}}$  applied on the structure shown in figure 1(a) by the magnetic field is [10]

$$T_{\text{field}} \cong WhLM_s H_{\text{ext}} \cos \theta, \quad (1)$$

where  $W$ ,  $h$  and  $L$  are the width, thickness and length of the ferromagnetic structure, respectively.  $M_s$  is the saturation magnetization.  $H_{\text{ext}}$  is the strength of the external magnetic field. As indicated in figure 1(b), a magnetic field is applied globally on the substrate. Thus, the movable metal structures can be lifted up by the magnetic force, and the movable structure supported by torsional springs has an equilibrium angular position between  $\theta_A$  ( $\theta_A = 0^\circ$ ) and  $\theta_D$  ( $\theta_D = 90^\circ$ ). At this particular angle, the net torque resulted from the magnetic field and the torsional springs is zero. Hence, the angular position of the movable structure can be tuned by either the spring stiffness or  $H_{\text{ext}}$ . On the other hand, the movable structure supported by hinges has only one equilibrium position at  $\theta_D$ .

The most important characteristic of this study is the localized heating of the magnetic film using the high-frequency time varying magnetic field. The high-frequency magnetic field will induce an eddy current on the magnetic film [11]. Thus, the magnetic material will be heated by a so-called induction heating technique [12]. According to the Steinmetz

law [13], the time varying magnetic field will lead to power loss of the material, including hysteresis loss and eddy current loss. The hysteresis loss and eddy current loss vary linearly and quadratically with the frequency of the magnetic field, respectively. Thus, the eddy current loss will dominate the power loss at the high-frequency magnetic field. As a result, the temperature-increasing rate  $\dot{T}$  of the material due to the high-frequency magnetic field is expressed as

$$\dot{T} \cong C(Bf)^2, \quad (2)$$

where  $C$  is the material and geometry constant of the film,  $B$  is the magnetic flux density and  $f$  is the frequency of the magnetic field. The magnetic flux density  $B$  can also be expressed as

$$B = \mu H_{\text{ext}}, \quad (3)$$

where  $\mu$  is the permeability. According to equations (2) and (3), the rising temperature of the silicon substrate and the films varies quadratically with their relative permeability. This characteristic can be employed to define different temperature regions using the deposited films. In this study, the ferromagnetic material with a larger relative permeability is used to act as a heater.

As shown in figure 1, the time varying magnetic flux  $\Phi$  associated with the structure at angular position  $\theta$  is expressed as

$$\Phi = \mu H_{\text{ext}} WL \cos \theta = B \cdot A \cos \theta. \quad (4)$$

Therefore, the material and geometry constant  $C$  in equation (2) will vary with  $A \cos \theta$ , and the rising temperature of materials resulted from magnetic induction heating is proportional to the surface area of workpieces (Si substrate or thin film structures) that are orthogonal to the magnetic flux [14]. The surface area of the fixed heater is always orthogonal to the magnetic flux during assembly, as depicted in figure 1(b). The surface area of the movable plate is also orthogonal to the magnetic flux before assembly, as indicated by  $\theta_A$  in figure 1(b). However, the movable plate will drastically move to other angular positions when applying the magnetic field. Meanwhile, the surface area of the plate orthogonal to the magnetic field will decrease immediately. When the plate reaches the position near  $\theta_D$ , the area orthogonal to the magnetic field can even be ignored. Thus, the movable structure can be prevented from heating by the magnetic field. In addition, according to equation (4), the heater is designed to have a much larger surface area  $A$  than the other fixed components such as hinges and anchor pads. Hence, the rising temperature of the heater is also much higher than that of the other fixed components. In summary, the fixed heater made of magnetic film in figure 1(b) will act as a localized heating source to melt the solder. The movable structure in figure 1(b) will be lifted up and then positioned by the magnetic field first, and then assembled and welded to the solder.

### 3. Experiment and results

This study designed and fabricated two test structures to demonstrate the feasibility of the localized welding technology. The test structure illustrated in figure 1 comprised a movable plate fixed to the substrate by torsional springs

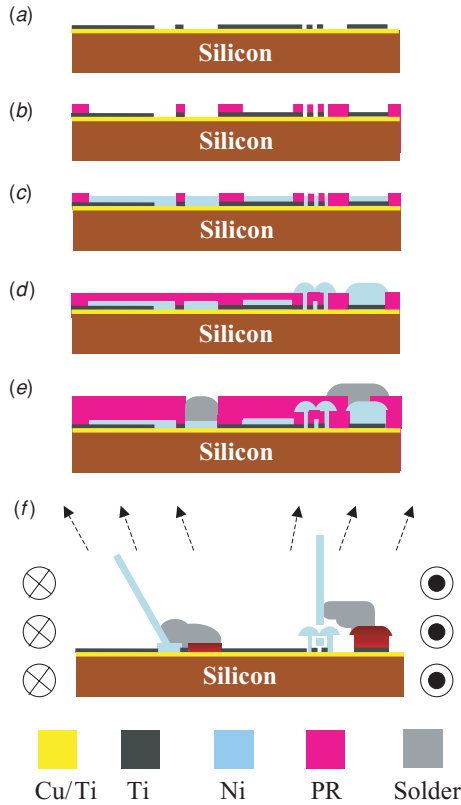


**Figure 2.** The fabrication process steps of the test structure.

(or hinges), and a solder was also attached to the plate. The fabrication processes of the test structure are shown in figure 2. First, the Cu/Ti films were evaporated on the Si wafer to act as the seed layer for electroplating. After that, the Ti film was selectively deposited using the lift-off process, as shown in figure 2(a). In figure 2(b), the photolithography was used to define the shape and dimensions of the micromachined structures. As shown in figure 2(c), the electroplated Ni was then employed to form the metal micromachined structures such as the movable plate, the torsional spring and the heater. The second photolithography and Ni electroplating processes in figure 2(d) were employed to fabricate the hinge. Hence, the photoresist acted as the spacer and sacrificial layer to define the space between two Ni layers. The final molding and electroplating processes in figure 2(e) defined the dimensions and location of the solder on the Ni plate. After removing the photoresist, part of the Ni test structures were ready to move. As shown in figure 2(f), these test microstructures will then be assembled and welded in the magnetic field. In this study, the electroplating solutions for the Ni and Sn/Pb solder are summarized in table 1; moreover, the typical applying magnetic power was 21 kW and the rising temperature of the heater was near 190 °C.

As indicated in figure 2(c), this study employed the Ti and Cu films as seed layers during electroplating. The Ti seed layer has a poor adhesion with the electroplated Ni film. This study selected the Ti film to ease the separation of movable Ni structures and substrate. Through this manner, the movable Ni structures were even freely to move without the releasing process. On the other hand, the fixed ends of the torsional

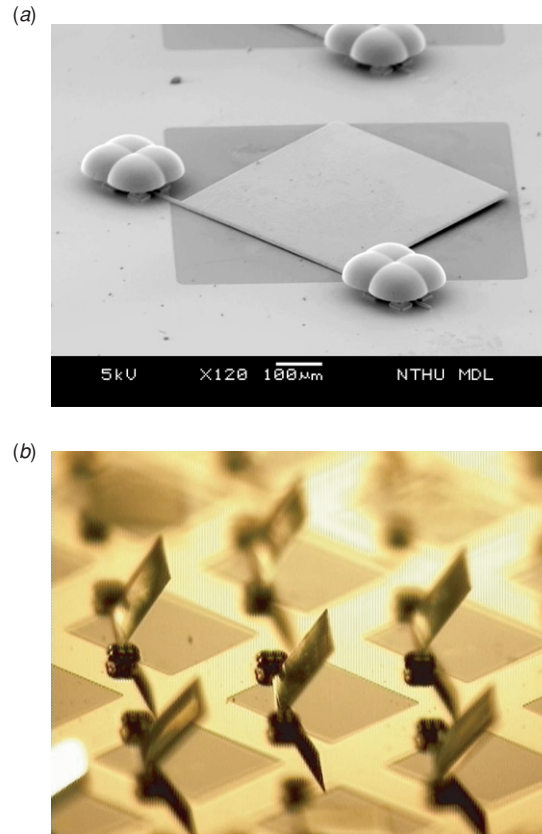


**Figure 3.** (a) The test structure used to evaluate the separation of Ti and Ni films, and (b) it was easy to separate Ni plates with Ti film by merely applying the magnetic field.

**Table 1.** The recipe of electroplating solutions for (a) the Ni/Co and (b) the Pb/Sn solder layer.

(a) Plating solution for the electroplating of nickel	
Nickel sulfamate $\text{Ni}(\text{NH}_2\text{SO}_4)_2 \cdot 4\text{H}_2\text{O}$	450–550 $\text{ml l}^{-1}$
Nickel chloride $\text{NiCl}_2 \cdot 6\text{H}_2\text{O}$	2–7 $\text{g l}^{-1}$
Boric acid $\text{H}_3\text{BO}_3$	30–50 $\text{g l}^{-1}$
Stress reducer	2–10 $\text{ml l}^{-1}$
(b) Plating solution for the electroplating of Sn/Pb solder	
Tin	12–18 $\text{g l}^{-1}$
Lead	1.5–2.5 $\text{g l}^{-1}$
pH value	3.0–5.0
Specific weight	1.1–1.2

spring, the hinges and the heater needed to anchor at the substrate. Hence, the Cu seed layer was selected to ensure a better adhesion of anchored Ni structures and substrate.

The SEM photo in figure 3(a) shows a Ni beam and its hinges. This test structure was used to evaluate the separation of Ti and Ni films. It is visible that the Ni plate is separated from the Ti film underneath, whereas the Ni hinges still properly attach to the substrate through the Cu seed layer. It was easy to lift up these plates after applying a magnetic field during assembly, as shown in figure 3(b). Figure 4 shows the SEM photos of two typical fabricated structures before welding. Figure 4(a) shows a beam supported by torsional springs, and figure 4(b) shows a movable plate constrained to the substrate by hinges. The Ni heater and the solder are also clearly observed in the SEM photos. The SEM photo in

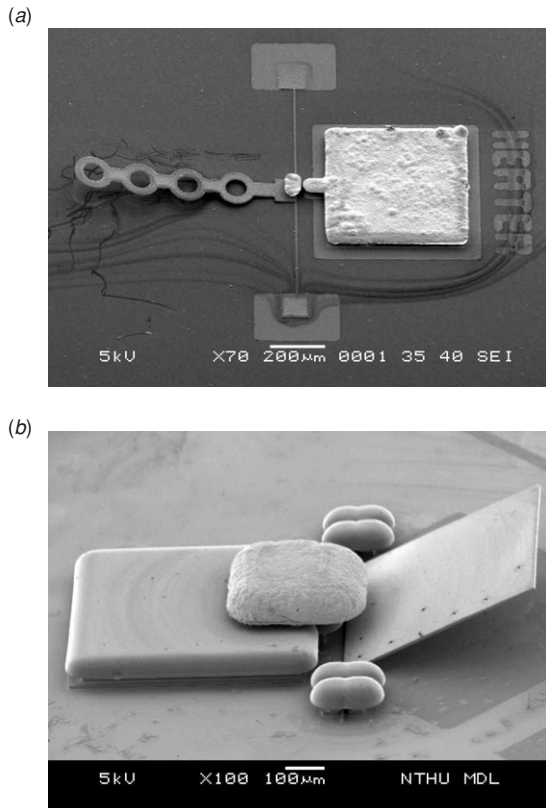


**Figure 4.** SEM photos of two typical fabricated structures before welding: (a) a beam supported by torsional springs and (b) a movable plate constrained to the substrate by hinges.

figure 5(a) shows the beam in figure 4(a) after assembly. The photo in figure 5(b) shows the close-up of the welding position. The SEM photo in figure 5(c) shows the plate in figure 4(b) after assembly. The results have demonstrated that the present welding technique is a simple and promising approach for wafer level assembly of microstructures.

#### 4. Discussions

In this study, the magnetic field was employed not only to lift up the structures but also to heat the solder and to weld the structures. Hence, a high-frequency magnetic field was required. After fabricating the structures in figure 4(a), an ac magnetic field was applied on the substrate to conduct the assembly process. In general, the ac magnetic field will induce an oscillation of the structure supported by torsional springs, so that the position of the structure could be influenced during assembly. The measurement results in figure 6 show the variation of the oscillation amplitude with the driving frequency  $f$  of the magnetic field. Apparently, the oscillation amplitude of the structure was drastically decreased with increasing driving frequency  $f$ . The oscillation angle of the structure was approximately zero when the driving frequency  $f$  is above 100 Hz. The inset in figure 6 indicates that the driving signal is regarded as dc for a high driving frequency  $f$ . According to equation (2), increasing the frequency  $f$  of the magnetic field will increase the rising temperature of induction heating. In general, the magnitude field is operated at the

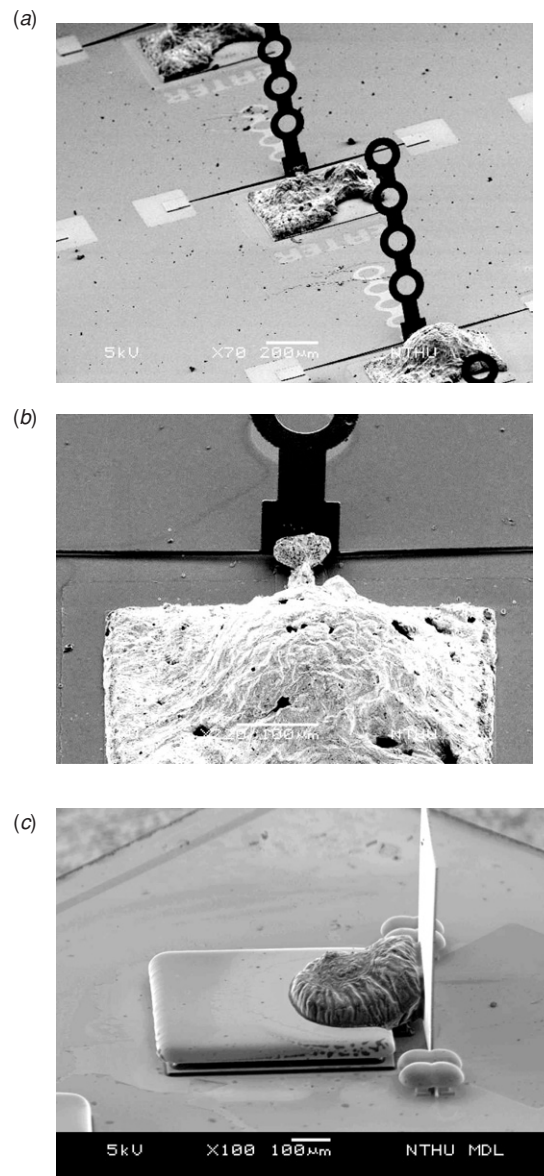


**Figure 5.** SEM photos of the structures in figure 4 after welding: (a) the beam in figure 4(a), (b) the zoom-in photo to show the welding point and (c) the movable plate in figure 4(b).

frequency range of 30 kHz to 3 MHz during induction heating [9]. Consequently, the oscillation of the plate is ignored under the above operation frequency range.

Figure 7 shows the angular displacement of the beam in figure 4(a) for different magnetic powers at a frequency  $f$  of 100 Hz. The data points in figure 7 indicate the static-equilibrium position of the beam resulted from the moments of the torsional spring restoring force, the gravity force and the magnetic lift-up force. According to equation (1), the torque  $T_{\text{field}}$  applied on the structure is decreased when the angular displacement  $\theta$  is increased. Thus, the angular displacement of the beam with torsional springs was converged to a particular position. The test structure in figure 7 was lifted up for  $53^\circ$  when the driving magnetic power reached 27 kW. However, the structure supported by hinges does not experience a spring restoring force. It acts as an invert pendulum on the silicon substrate, and has an equilibrium position at the magnetic field

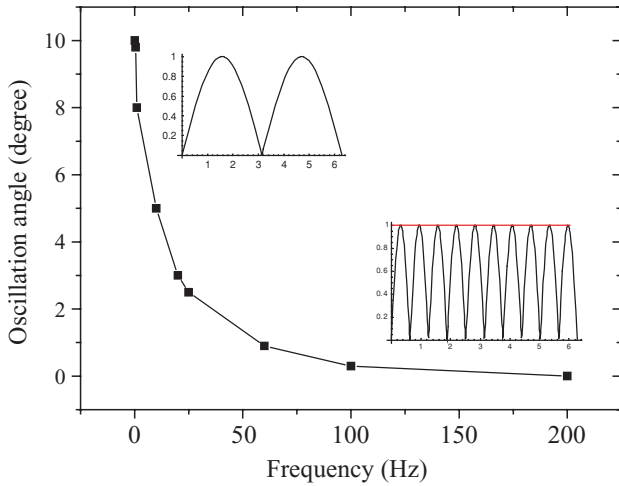


**Figure 6.** The measured variation of the oscillation amplitude with the driving frequency  $f$  of the magnetic field.

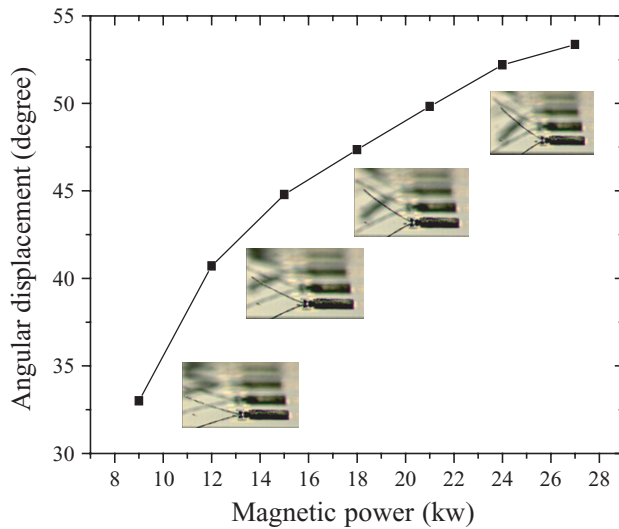


**Figure 7.** The measured angular displacement of the beam (in figure 4(a)) for different driving voltages; the driving frequency  $f$  is 100 Hz.

when  $\theta = 90^\circ$ . Thus, the plate in figure 4(b) was lifted up to near  $90^\circ$ , as shown in figure 5(c).

The silicon substrate and the thin film structures will be heated by magnetic loss. The hysteresis curve of the movable electroplated Ni microstructure in figure 8 was measured using the vibrating sample magnetometry. The small area within this curve further demonstrates that the hysteresis loss can be ignored. In this study, the nickel film which is a ferromagnetic material with a relative permeability of  $100 \text{ H m}^{-1}$  was used as a heater. However, the silicon substrate had not been heated since it is a diamagnetic material with relative permeability approximately zero [10]. As shown in figure 4, the heater was designed to have a larger surface area; in addition, the surface area of the heater was always orthogonal to the magnetic flux during assembly. Hence, the rising temperature of the heater was much higher than that of the other components. Figure 9 shows typical temperature distribution of the heater measured by an infrared microscope. The rising temperature of the heater was  $190^\circ\text{C}$  in 15 s, when the applying magnetic power

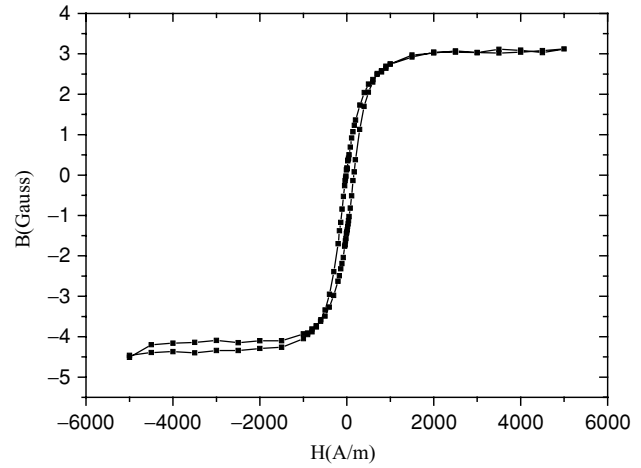


**Figure 8.** The hysteresis curve of the movable electroplated nickel microstructure measured using the vibrating sample magnetometry.

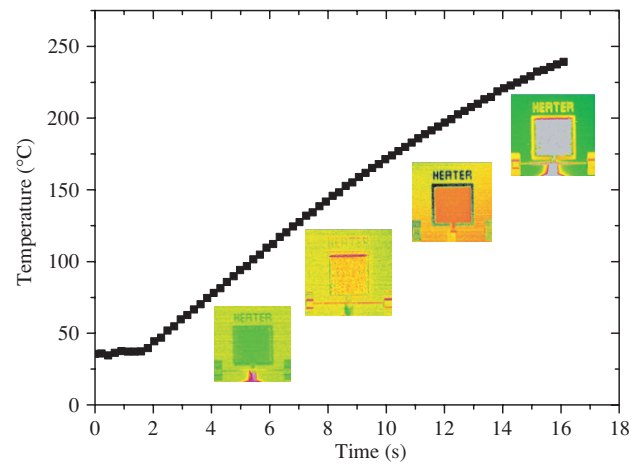


**Figure 9.** Typical temperature distribution of the heater for various heating times measured by an infrared microscope.

was 21 kW. The insets in figure 9 also indicate that the heater had a higher rising temperature, so that the localize induction heating can be achieved.

## 5. Conclusions

This study has successfully demonstrated a process to localize, assemble and weld microstructures using an external magnetic field. In this study, the magnetic field is not only to assemble the microstructures but also to fix them by induction welding. The assembly and welding can be localized at a particular position by a global magnetic film. In this manner, a wafer level process can be achieved by the global magnetic field. In addition, the heating temperature can be easily tuned by varying the area of the magnetic film. Thus, photolithography can define various temperature regions on a substrate. This characteristic is especially useful for devices implemented using planar fabrication processes.

## Acknowledgments

This project was (partially) supported by the NSC of Taiwan under grant of NSC-93-2218-E-007-012, and the Ministry of

Economic Affairs, Taiwan, under contract no 93-EC-17-A-07-S1-0011. The authors would also like to thank the NSC Central Regional MEMS Center (Taiwan), the Nano Facility Center of National Tsing Hua University and the NSC National Nano Device Laboratory (NDL) for providing the fabrication facilities.

## References

- [1] Romankiw L T 1997 A path from electroplating through lithographic masks in electronics to LIGA in MEMS *Electrochim. Acta* **42** 2985–3005
- [2] Cohen A, Zang G, Tseng F G, Mansfeld F and Will P 1999 EFAB: rapid, low-cost desktop micromachining of high aspect ratio true 3-D MEMS *Proc. IEEE MEMS'99 Workshop (Orlando, FL)* pp 244–51
- [3] Pister K S, Judy M W, Burgett S R and Fearing R S 1992 Microfabricated hinges *Sensors Actuators A* **33** 249–56
- [4] Ho Y P, Wu M, Lin H-Y and Fang W 2004 A robust and reliable stress-induced self-assembly supporting mechanism for optical devices *Microsyst. Technol.* **11** 214–20
- [5] Yi Y W and Liu C 1999 Magnetic actuation of hinged microstructures *IEEE J. Microelectromech. Syst.* **8** 10–7
- [6] Kaajakari V and Lal A 2001 Electrostatic batch assembly of surface MEMS using ultrasonic triboelectricity *Proc. IEEE MEMS'01 Workshop (Interlaken, Switzerland, 10–13 Jan.)*
- [7] Harsh K F, Irwin R S and Lee Y C 1998 Solder self-assembly for MEMS *Proc. 1998 Int. Instrumentation Symp. (ISA 98) (Reno, NV)* pp 256–61
- [8] Syms R R A 1999 Surface tension powered self-assembly of 3-D micro optomechanical structures *J. Microelectromech. Syst.* **8** 448–55
- [9] Yang H A and Fang W 2005 On the scale effect of magnetic induction heating for microstructure *Transducers'05 (Seoul, Korea)* pp 2123–6
- [10] Miller R A and Tai Y C 1997 Micromachined electromagnetic scanning mirrors *Opt. Eng.* **36** 1399–407
- [11] Cullity L C 1972 *Introduction to Magnetic Materials* (Reading, MA: Addison-Wesley)
- [12] Cable L C and Wesley J 1954 *Induction and Dielectric Heating* (New York: Reinhold)
- [13] Steinmetz C P 1915 *Theoretical Elements of Electrical Engineering* 4th edn (New York: McGraw-Hill)
- [14] Jackson J D 1975 *Classical Electrodynamics* 2nd edn (New York: Wiley)